Published in final edited form as:

Adv Funct Mater. 2016 June 14; 26(22): 4016–4025. doi:10.1002/adfm.201504184.

Multifunctional Magnetic Particles for Combined Circulating Tumor Cells Isolation and Cellular Metabolism Detection

Jiao Wu,
Center for Bio-Nano-Chips and Diagnostics in Translational Medicine (CBD™), School of Biomedical Engineering, Med-X Research Institute and Shanghai Chest Hospital, Shanghai Jiao Tong University, Shanghai 200030, China

Xiang Wei,
Center for Bio-Nano-Chips and Diagnostics in Translational Medicine (CBD™), School of Biomedical Engineering, Med-X Research Institute and Shanghai Chest Hospital, Shanghai Jiao Tong University, Shanghai 200030, China

Jinrui Gan,
Department of Chemistry, Institute of Biomedical Sciences and State Key Lab of Molecular Engineering of Polymers, Fudan University, Shanghai 200433, China

Lin Huang,
Center for Bio-Nano-Chips and Diagnostics in Translational Medicine (CBD™), School of Biomedical Engineering, Med-X Research Institute and Shanghai Chest Hospital, Shanghai Jiao Tong University, Shanghai 200030, China

Ting Shen,
NanoLite Systems, Austin, TX 78795, USA

Prof. Jiatao Lou,
Center for Bio-Nano-Chips and Diagnostics in Translational Medicine (CBD™), School of Biomedical Engineering, Med-X Research Institute and Shanghai Chest Hospital, Shanghai Jiao Tong University, Shanghai 200030, China

Prof. Baohong Liu,
Department of Chemistry, Institute of Biomedical Sciences and State Key Lab of Molecular Engineering of Polymers, Fudan University, Shanghai 200433, China

Prof. John X.J. Zhang, and
Thayer School of Engineering, Dartmouth College, NH 03755, USA

Prof. Kun Qian
Center for Bio-Nano-Chips and Diagnostics in Translational Medicine (CBD™), School of Biomedical Engineering, Med-X Research Institute and Shanghai Chest Hospital, Shanghai Jiao Tong University, Shanghai 200030, China

John X.J. Zhang: john.zhang@dartmouth.edu; Kun Qian: k.qian@sjtu.edu.cn

Correspondence to: John X.J. Zhang, john.zhang@dartmouth.edu; Kun Qian, k.qian@sjtu.edu.cn.

Supporting Information

Supporting Information is available from the Wiley Online Library or from the author.

Abstract

We for the first time demonstrate multi-functional magnetic particles based rare cell isolation combined with the downstream laser desorption/ionization mass spectrometry (LDI-MS) to measure the metabolism of enriched circulating tumor cells (CTCs). The characterization of CTCs metabolism plays a significant role in understanding the tumor microenvironment, through exploring the diverse cellular process. However, characterizing cell metabolism is still challenging due to the low detection sensitivity, high sample complexity, and tedious preparation procedures, particularly for rare cells analysis in clinical study. Here we conjugate ferric oxide magnetic particles with anti-EpCAM on the surface for specific, efficient enrichment of CTCs from PBS and whole blood with cells concentration of 6–100 cells per mL. Moreover, these hydrophilic particles as matrix enable sensitive and selective LDI-MS detection of small metabolites (MW<500 Da) in complex bio-mixtures and can be further coupled with isotopic quantification to monitor selected molecules metabolism of ~50 CTCs. Our unique approach couples the immunomagnetic separation of CTCs and LDI-MS based metabolic analysis, which represents a key step forward for downstream metabolites analysis of rare cells to investigate the biological features of CTCs and their cellular responses in both pathological and physiological phenomena.

Graphical Abstract

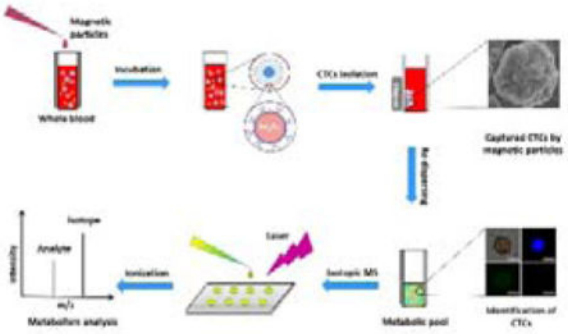

The characterization of circulating tumor cells (CTCs) metabolism plays a significant role in understanding the tumor microenvironment, through exploring the diverse cellular process. Herein, multi-functional magnetic particles are developed for combined rare cell isolation and downstream laser desorption/ionization mass spectrometry to measure the metabolism of enriched CTCs.

Keywords

magnetic particles; circulating tumor cells (CTCs); surface conjugation; laser desorption/ionization mass spectrometry; small metabolites

1. Introduction

The rising engagement of magnetic particles in biomedical applications is strongly correlated to their key properties including physical structures, surface chemistry, and magnetic material parameter.[1] For magnetic separation, through tuning the surface chemical property of magnetic particles, various biological targets ranging from nano- to

micro- scale can be selectively captured for therapeutic and diagnostic studies. In addition, the magnetic property of particles is crucial for the throughput and yield of separation in real applications. Particularly, the functionalized magnetic particles can be designed to specifically bind biomolecules for either immuno-isolation of living cells[1e, 2] or molecular profiling and detection.[1a, 3] Meanwhile, laser desorption/ionization mass spectrometry (LDI MS) has become a fundamental tool for molecular analysis by molecule weights (MW) allowing facile sample preparation, fast analytical experiments, and accurate structural identification.[4] In LDI MS, magnetic particles can not only serve as chemo-specific materials for enrichment of target proteome/peptidome during sample pre-treatment,[1a, 3a–c] but also facilitate the LDI process for detection without the use of common organic matrix.[1a, 4a, 5] It is noted that most current efforts in magnetic particles based LDI MS are focused on detection of bio-macromolecules like proteins and peptides, the application of magnetic particles dealing with small metabolites (MW<500 Da) is yet to be explored for current metabolic analysis in cell research.

Cell metabolism is a dynamic process, which is crucial to reveal the intrinsic and extrinsic features of cells and investigate the cellular behavior in pathological and physiological phenomena.[6] However, characterizing cell metabolism is still challenging due to the low detection sensitivity, high sample complexity and tedious preparation procedures, particularly for rare cells analysis in clinical study.[6a, 7] In a case of circulating tumor cells (CTCs), blood-borne rare cells shed from the primary tumors, current full range of CTCs molecular characterization includes proteomic (e.g. immuno-fluorescence) and genetic strategies (such as fluorescence in situ hybridization and quantitative RT-PCR) to detect proteins and nucleic acids, respectively.[2a, 2b, 8] Despite that, metabolism study of CTCs is largely hindered without a designer platform combining appropriate multiple analytical techniques, but can contribute to a new understanding of cancer metastasis and therapy resistance and to advances in precision medicine.[9] Therefore, invention of a new method is of great significance to address the challenges in the characterization of rare cells metabolism and will play a paramount role for the progress of tumor research.

It should be noted that CTCs exist at extremely low abundance with one CTC in every one billion blood cells in the peripheral blood of patients.[10] Besides, their low recovery in downstream detection also poses a serious obstacle for CTCs isolation and analytical systems.[2c, 11] In recent years, many approaches have been developed to selectively enrich CTCs according to their physical and chemical properties.[2b, 10, 12] To date, immunoassays are most commonly adapted to provide desirable capture specificity and efficiency by utilizing epithelial cell adhesion molecule (EpCAM) and its antibody.[2c, 10a, 13] For one example, satisfying the needs for high throughput, standardization, and easy operation, immunomagnetic particles based CellSearch™ platform serves as the only system approved by Food and Drug Administration in US for clinical CTCs analysis.[14] Nevertheless, immunomagnetic particles require rational design with multiple functions to facilitate the novel metabolic downstream analysis and maximize the therapeutic and diagnostic value of CTCs in clinics.[7]

Previously we have reported particle assisted laser desorption/ionization mass spectrometry (PALDI MS) for small metabolites analysis from biological samples[4a, 15] and

immunomagnetic assays for efficient CTCs isolation in blood.[2a, 2b, 16] Herein, we demonstrated the combination of rare cell isolation and PALDI MS to detect the metabolism of captured CTCs for metabolic study based on functional ferric oxide magnetic particles (Figure 1). The magnetic particles were surface modified by anti-EpCAM for selective enrichment of CTCs and more importantly, these particles served as ideal matrix for LDI MS due to their nanoscaled size, stable structure, hydrophilic surface, and strong UV-light absorption. Consequently, sensitive PALDI MS analysis can be achieved towards various small metabolites from complex bio-mixture due to the unique selective LDI process. Further isotope assisted quantification was coupled to investigate small molecules metabolism of ~50 CTCs. This work starts a facile designer technology for downstream metabolic analysis of CTCs and provides new insights towards characteristics of rare cells in diverse dynamic biological process.

2. Results and discussion

2.1. Preparation and characterization of functional magnetic particles

The functional ferric oxide particles were prepared by surface conjugation with anti-EpCAM, where the biotinylated anti-EpCAM was linked to streptavidin coated magnetic particles through biotin-streptavidin interaction as reported.[16a] As shown in Figure 2a, TEM demonstrated that the particles had a diameter of ~200 nm (as previous selected)[2b] and were composed of ultra-small magnetic nanocrystals (size of 3–6 nm). A coated layer can be observed with thickness ~6–10 nm compared to the untreated particles (Figure S1a) due to surface functionalization. DLS of the particles in Figure 2b displayed a narrow size distribution with an increased average diameter of 220.6 nm and polydispersity index (PDI) of 0.090 after surface functionalization (compared to Figure S1b), agreed to SEM (Figure 3a and Figure S1c) and TEM and suggesting their fine dispersity in solution for both cell capture and LDI matrix use.

Besides, the magnetic hysteresis loop of anti-EpCAM coated particles indicated their saturation magnetization value of 18.76 emu/g without remanence (lower than that of the initial particles in Figure S2a, owing to surface conjugation[17]), when cycling the field between −20 kOe and 20 kOe. These particles can be quickly separated by a commercial permanent magnet in 40 s (inset of Figure 2c) due to the fast response of magnetic nanoparticles. It should be mentioned that the ferric oxide particles exhibited strong absorption around 280–1100 nm before and after the modification process (Figure 2d and S2b), which would be critical for LDI MS detection.[4a, 5a, 15a] The desirable size, stable structure, fine solution dispersity, superparamagnetic property and UV-light absorption of the particles are essential for facile rare cell separation and a designed integration with LDI MS detection.

2.2. Capture and identification of CTCs by immunomagnetic assays

In the following CTCs capture experiments using MCF-7 cells (from human breast cancer, EpCAM positive) as targets, the pristine cells were shriveled to a size of ~8 μm due to the drying process under SEM observations (Figure 3b). For comparison, cell surface was densely decorated by particles (Figure 3c and the zoomed image of particles on cell surface

in Figure 3d) after the immuomagnetic separation. For identification and screening experiments, fluorescence staining was performed to discriminate CTCs from non-specific cells (e.g. white blood cells) as previously reported.[2a, 16a] For a typical captured CTC, the bright field image illustrated a near-spherical shape of the cells with particles labeled cell surface on the edge area in accordance with SEM (Figure 4a). The cells with fluorescence images displaying positive for DAPI (Figure 4b,blue color) and CK (Figure 4c, green color from FITC) and negative for CD45 (Figure 4d, red color from cy3) were identified as MCF-7 cells, which were similar to literatures. On the contrary, the cells with fluorescence staining results showing DAPI+/CK−/CD45+ were identified as white blood cells (Figure S3a–d).

Based on the above fluorescent analysis of each individual cell as captured, efficiency of the immunomagnetic assay can be determined by spiked experiments (see Experimental Section for details). Over 99% and 85% of CTCs can be simply isolated from PBS buffer and whole blood, respectively (Figure 4e), by the use of functional magnetic particles for separation without any other devices except for a magnet. For selectivity test in Figure 4f, over 99% of MCF-7 cells (EpCAM postive) can be enriched through the immunomagnetic assay, whereas the nonspecific ratio was merely less than 3% in the case of Hela cells (EpCAM negative), evidencing the highly specific binding nature of the EpCAM modified particles. Moreover, the capture efficiencies for lower cell concentrations were investigated by spiking experiments in PBS and whole blood. Given the concentration ranging from 12 to 60 cells mL^{-1}, over ~90% and ~82% of cells were captured in PBS buffer (Figure 3g) and whole blood (Figure 3h), respectively. With the concentration lowered to 6 cells mL^{-1}, the capture rate still reached 72% in PBS and 66% in whole blood, suggesting that the functional particles can be effectively applied to capture cancer cells in real case. All these results demonstrated that our method can capture tumor cells with high sensitivity and has comparable results with current reports using magnetic particles or other techniques for rare cells separation.[2d, 8b, 18] Hence, successful launching of the immunomagnetic assays and identification of CTCs had been validated in different concentrated cells systems promising the next steps of cellular metabolism analysis.

2.3. Detection of small metabolites using the magnetic particles

These functional magnetic particles can not only be used as a specific labeling reagent for CTCs isolation, but also contribute to efficient LDI MS detection of small metabolites. As displayed in Figure 5a-i, no molecular peaks can be viewed from a standard metabolites mixture (containing glucose, sucrose, phenylalanine and glutamic acid) without any matrix suggesting the very low LDI efficiency. When conventional CHCA was applied (Figure 5b-i), strong interference signals appeared in the low mass range (<500 Da) and only weak peaks of metabolites can be observed due to the fragmentation and interference of organic matrix.[4a, 5a] In parallel, group of specific peaks from small molecules can be obtained in Figure 5c-i and the inset without background noise, yielding m/z 203.04$[M+Na]^+$ and m/z 219.02$[M+K]^+$ for glucose, m/z 365.09$[M+Na]^+$ and m/z 381.06$[M+K]^+$ for sucrose, m/z 188.06$[M+Na]^+$ and m/z 204.04$[M+K]^+$ for phenylalanine, and m/z 170.04$[M+Na]^+$ and m/z 186.01$[M+K]^+$ for glutamic acid (See also Figure S4 for the LDI MS results of each standard molecule using the particles and Table S1 for the accurate masses with detection-

of-limits measured). These results revealed the high performance of these particles in small metabolites detection due to their desirable structural parameters as characterized in Figure 2, which is comparable to the current reports and materials in LDI MS.[4a, 5a, 5b, 15a, 19]

Further we demonstrated the selective LDI of small metabolites[15a] by the particles from complex bio-mixtures. In control experiments, no small molecules can be detected in a peptides mixture (Figure 5a-ii and S5a&d) and proteins (Figure 5a-iii and S6a&d) mixtures without any matrix in the low mass range due to low LDI efficacy. In contrast, the peptides and proteins can be well recognized by the use of CHCA matrix as shown in Figure 5b-ii (also Figure S5b&e) and 5b-iii (also Figure S6b&e), respectively. When the magnetic particles were employed, the peptides/proteins cannot be detected (Figure 5c-ii&ciii, S5c&f, S6c&f) and the small metabolites can be well identified in mixtures (the insets of Figure 5c-ii&ciii, S5c&f, S6c&f). These results validated the magnetic particles were able to selectively enhance the LDI efficiency of small metabolites in diverse peptides/proteins bio-mixtures during MS analysis superior to traditional organic matrix, which is advantageous for their applications in metabolic detection of bio-samples with high sample complexity in nature.

2.4. Isotopic assisted LDI MS analysis of CTCs metabolism

In the final stage, we implemented combined CTCs isolation and cellular metabolism detection using the immunomagnetic particles. No signals from metabolites can be observed by direct LDI MS of ~50 pristine MCF-7 cells without matrices (Figure 6a), whereas strong background signals can be found in the spectra and detection was failed using the traditional organic matrix (Figure S7). For comparison, series of specific peaks from small metabolites can be viewed by the direct LDI MS of ~50 captured MCF-7 cells with magnetic particles as matrix (for instance, m/z 203.04$[M+Na]^+$ and m/z 219.02$[M+K]^+$ for glucose in Figure 6b) due to the unique selective LDI process as demonstrated by our previous steps (Figure 5 and Figure S5 and S6), showing the key role of magnetic particles for both immunomagnetic assay and LDI MS. It should be noted that the peak intensity in LDI MS cannot be directly used for quantification purpose due to the non-predictable ionization behavior.[20] To investigate the metabolism velocity of the captured CTCs, the isotopic assisted technique was introduced (using isotopes of small molecules as the internal standard) in LDI MS for quantification.[19b, 19c] Typical MS spectra for metabolites detection using isotopic standards have been listed in the Figure 6c-j. The analyte/isotope ratio of glucose, sucrose, phenylalanine and glutamic acid were measured based on the $[M+Na]^+$ and its isotope peaks at m/z 204.04$[M+Na]^+$ for glucose isotope (Figure 6c and d), m/z 377.09$[M+Na]^+$ for sucrose isotope (Figure 6e and f), m/z 194.06$[M+Na]^+$ for phenylalanine isotope (Figure 6g and h), and m/z 173.04$[M+Na]^+$ for glutamic acid isotope (Figure 6i and j).

The as-measured intensity ratios revealed the content of metabolites and can be used to estimate the metabolism velocity of selected small metabolites. For cellular carbohydrates metabolism, Figure 7a revealed that glucose can be consumed over by ~50 CTCs after 24 h with analyte/isotope (a/i) ratio reduced from 0.604 to 0, while the metabolism velocity was much slower in the case of sucrose (a/i reduced from 0.707 to 0.503, Figure 7b). In parallel, for cellular amino acids metabolism, the metabolism velocity can also be quite distinct for

different molecules. The consumption of phenylalanine (a/i reduced from 0.751 to 0, Figure 7c) was much faster than that of glutamic acid (a/i reduced from 0.554 to 0.371, Figure 7d) by the CTCs. It should be noted that a blank control without any cell and a control group with normal cells were conducted to validate the above observations. For standard solutions without cells, the a/i ratio after 24 h remained the same as 0 h and no consumption of metabolites can be found for the four metabolites (Figure S8, 9). When normal white blood cells were evaluated using the same procedures for MCF-7 cells, we still did not observe any consumption of metabolites for the four metabolites (with a/i ratio unchanged, Figure S10, 11) due to the fact that the functional magnetic particles cannot target normal cells (EpCAM negative) for detection of metabolites. Therefore, we demonstrated unique performance of these particles in monitoring the metabolism of CTCs, which may provide new insights to cancer metastasis associated CTCs in clinics.[21] And we concluded that the functional magnetic particles bridged the immunomagnetic assay and LDI MS for efficient CTCs capture and metabolism study, where the metabolism velocity of various molecules can be studied during the downstream analysis of CTCs.

3. Conclusion

In summary, characterizing metabolism of CTCs reveals the virtual cellular process and complements the proteomic and genomic study of these rare cells. In this work, we for the first time combined CTCs isolation and cellular metabolism detection based on designed magnetic particles (Figure 1). The key features of our method can be concluded as follows: I) immunomagnetic particles with designed size, dispersity, magnetic response and functional surface (Figure 2a–c) for efficient capture of CTCs from spiked samples at low cells concentrations (Figure 3 and 4); II) stable structure of the particles with strong UV laser absorption (Figure 2a and 2d) for sensitive (Figure S4, Table S1) and selective LDI MS analysis of metabolites from complicated bio-mixtures (Figure 5, S5 and S6); III) isotopic quantification to monitor selected small molecules (e.g. carbohydrates and amino acids) metabolism of ~50 captured CTCs (Figure 6 and 7). This work represents a key step forward for rare cell analysis to explore the biological features of CTCs and investigate their cellular responses in diverse pathological and physiological process.

4. Experimental Section

Preparation of functional magnetic particles

Immunomagnetic particles were prepared by surface immobilization with anti-EpCAM. The initial magnetic particles (size of 200 nm) were synthesized by an in-solution approach and coated by polymers (Mix&Go from Anteo Diagnostic) to conjugate with streptavidin as reported.[22] Then the streptavidin modified magnetic particles were incubated with biotinylated anti-EpCAM (Abcam Inc., Cambridge, USA) for final functionalization. Briefly, 100 μL of streptavidin magnetic particles (10 mg/mL) were mixed with 50 μL of biotinylated anti-EpCAM (0.2 mg/mL) and gently shaken at room temperature for 1 hour. The activated particles were collected by magnetic separator and washed two times with phosphate buffered saline (PBS) to remove surplus antibodies. Then a blocking procedure was performed by adding 1 mL of blocking buffer (10% bovine serum albumin, BSA) to

avoid potential nonspecific interactions during cell isolation. Finally the blocked particles were washed with PBS containing 0.1% Tween 20 (PBST) for two times and stored in storage buffer (PBS containing 0.5% BSA, 0.5% Tween 20 and 0.02% ProClin 300) at a concentration of 1 mg/mL at 4 °C before use.

Characterization methods and techniques

Transmission election microscopy (TEM) images were recorded by a JEOL JEM-2100F TEM instrument. The samples were prepared by depositing 10 μL of particles suspension onto a copper TEM grid before observation. Scanning electron microscopy (SEM) analysis was performed on Hitachi S-4800 operating at 10 kV. The suspensions of particles/cells were deposited on silicon wafer and directly observed in the SEM device after drying at room temperature. Magnetic hysteresis loops were measured using a vibrating sample magnetometer (Quantum Design, Physical Property Measurement System). Dynamic light scattering (DLS) measurements were conducted on a Malvern Zetasizer Nano ZS instrument by dispersing the magnetic particles in water. Room temperature optical absorption spectra of the materials were obtained on an AuCy UV1900 spectrophotometer.

Immunomagnetic isolation of CTCs

Human breast cancer cell lines MCF-7 cells (EpCAM positive) and cervical cancer cell lines Hela cells (EpCAM negative) were used as rare cells models to determine the efficiency and specificity of immunomagnetic assay in our work. These cells were maintained as reported in modified media consisting of high-glucose DMEM medium supplemented with fetal bovine serum (FBS), penicillin and streptomycin. To harvest cells, 1 mL of trypsin (0.25%) was dropped into flask for 5 min digestion in the CO_2 incubator and the obtained cells were washed with PBS buffer for two times. Cells counting were performed using trypan blue and hemocytometer under the microscopy (Olympus CKX 41). Both PBS buffer and whole blood were utilized to re-suspend the cells during the spiked experiments. All of the investigation protocols in this study were approved by the institutional ethics committee of the Shanghai Chest Hospital and School of Biomedical Engineering, SJTU. Written informed consents were obtained since the project started. For selective cell enrichment, 100 μL of as-prepared particles (1 mg/mL) were added to the system (2 mL of PBS with 5% BSA or 2 mL of whole blood) containing ~200 MCF-7/Hela cells spiked before. For cell isolation at lower concentration, from 6 to 60 cells were spiked in 1 mL PBS or whole blood. After incubating the mixture by gently shaking at 37 °C for 1 hour, magnetic particles labeled cells were collected by magnetic separator, washed two times and re-suspended in 100 μL of PBS before cell counting. By using the fluorescence staining, the number of captured cells is N. Then the capture rate can be calculated through the Equation 1 listed as below.

$$\text{Capture rate} = \frac{N}{200} \times 100\% \quad (1)$$

LDI MS of small metabolites

In LDI MS, using organic matrix, α-cyano-4-hydroxycinnamic acid (CHCA) solution (50/50/0.1, v/v/v, water/acetonitrile/trifluoroacetic acid) was prepared at a concentration of 10 mg/mL. 500 nL analytes solution was pipetted on the plate and dried at the room temperature. Then 500 nL of matrix solution was dropped on the plate and dried for LDI MS analysis. For LDI MS using magnetic particles, these particles were dispersed in water at a concentration of 1 mg/mL. Then 500 nL matrix slurry was prepared after dropped 500 nL of analytes solution on the plate and dried for LDI MS analysis. Standard small molecules (>99.99% purity) were purchased from SinaPharm Chemical Regent (Beijing) and Sigma-Aldrich (USA). The peptides (from protein digests) and proteins mixtures were prepared using established methods.[20b, 23] Mass spectra were acquired in the positive reflection mode on 5800 Proteomics Analyzer (Applied Biosystems) with the Nd:YAG laser at 355 nm, a repetition rate of 200 Hz and an acceleration voltage of 20 kV. All spectra were used as recorded without any smoothing and the delay time was optimized to be 500 ns in the experiments. Only MS signals with signal-to-noise ratio over 10 were used for identification of molecules based on accurate mass measurement (± 10 mDa).[15a, 24] No smooth spectra were used and all spectra were directly used for analysis.

Downstream analysis of CTCs

In cell counting and identification, the fluorescence staining method was employed by the use of 4′,6-diamidino-2-phenylindole (DAPI, Vector Laboratories Inc., UK), anti-Cytokeratin (CK) pan FITC (Sigma Aldrich Co., USA), and cy3 labeled anti-CD45 (Biorbyt, USA). Briefly, captured cells were dispersed in PBS and dropped on a glass slide for drying at 37 °C for 2 hours. Subsequently, excessive ice-cold acetone was introduced to the glass slides to fix the cells. Then the cells were stained with DAPI, anti-CK pan FITC, and cy3 labeled anti-CD45. Additionally, the fluorescence images of white blood cells were examined as control. Cells that had round to oval morphology and positive for DAPI (specific for DNA) and CK (a marker for epithelial cells) and negative for CD45 (expressed in leukocytes) were identified as MCF-7 cells, while cells positive for DAPI and CD45 and negative CK were identified as white blood cells.

In the detection of cellular metabolism, cells captured by magnetic particles were dispersed at a concentration of 50 cells/μL in buffer solution containing small metabolites including sugar molecules (glucose, sucrose) and amino acids (glutamic acid, phenylalanine). Typically, 1 μL of mixture containing ~50 cells was deposited on the plate and dried at the room temperature for direct LDI MS analysis on 5800 Proteomics Analyzer similar to the previous step. Then the mixture was analyzed by LDI MS using the magnetic particles as matrix for cellular metabolism analysis and isotopic quantification was employed based on the peak intensity ratio of analytes and isotopic internal standards.[19b, 19c] Fixed amounts of isotopes were added and the peak intensity ratio was measured before and after 24 h incubation. Five independent experiments were conducted in parallel to measure the signal ratios and the isotopic internal standards of small metabolites (labeled with ^{13}C or D) were purchased from Cambridge Isotope Laboratories (CIL), USA. For control groups, both standard solutions without any cell and normal white blood cells were employed in experiments. All the four metabolites including glucose, sucrose, glutamic acid, and

phenylalanine were tested and the same experimental procedures as the CTCs were conducted for the cells isolation and metabolism detection.

Supplementary Material

Refer to Web version on PubMed Central for supplementary material.

Acknowledgments

We gratefully thank the financial support from Project 81401542, 81550110257, 21175028, and 21375022 by National Natural Science Foundation of China (NSFC). This work is also sponsored by Shanghai Pujiang Program (14PJ1405100) and The Program for Professor of Special Appointment (Eastern Scholar) at Shanghai Institutions of Higher Learning (TP2015015). We are grateful for the financial support from the National Institute of Health (NIH) National Cancer Institute (NCI) Cancer Diagnosis Program under grant 1R01CA139070, during which period the immunomagnetic rare cell screening protocol was originally developed, and was later transferred to NanoLite Systems for pre-clinical evaluations.

References

1. a) Li Y, Zhang X, Deng C. Chem Soc Rev. 2013; 42:8517. [PubMed: 23933677] b) Häfeli, U.; Schütt, W.; Teller, J.; Zborowski, M. Scientific and clinical applications of magnetic carriers. Springer Science & Business Media; 2013. c) Akbarzadeh A, Samiei M, Davaran S. Nanoscale Res Lett. 2012; 7:1. [PubMed: 22214494] d) Ghosh D, Lee Y, Thomas S, Kohli AG, Yun DS, Belcher AM, Kelly KA. Nat Nanotechnol. 2012; 7:677. [PubMed: 22983492] e) Laurent S, Forge D, Port M, Roch A, Robic C, Vander Elst L, Muller RN. Chem Rev. 2008; 108:2064. [PubMed: 18543879] f) Dobson J. Gene Ther. 2006; 13:283. [PubMed: 16462855] g) Wang FB, Rong Y, Fang M, Yuan JP, Peng CW, Liu SP, Li Y. Biomaterials. 2013; 34:3816. [PubMed: 23465488]
2. a) Chen P, Huang YY, Hoshino K, Zhang JX. Sci Rep. 2015:5.b) Chen P, Huang YY, Hoshino K, Zhang XJ. Lab Chip. 2014; 14:446. [PubMed: 24292816] c) Ozkumur E, Shah AM, Ciciliano JC, Emmink BL, Miyamoto DT, Brachtel E, Yu M, Chen PI, Morgan B, Trautwein J, Kimura A, Sengupta S, Stott SL, Karabacak NM, Barber TA, Walsh JR, Smith K, Spuhler PS, Sullivan JP, Lee RJ, Ting DT, Luo X, Shaw AT, Bardia A, Sequist LV, Louis DN, Maheswaran S, Kapur R, Haber DA, Toner M. Sci Transl Med. 2013; 5:179.d) Min H, Jo SM, Kim HS. Small. 2015; 11:2536. [PubMed: 25630488] e) Jo SM, Lee JJ, Heu W, Kim HS. Small. 2015; 11:1975. [PubMed: 25504978]
3. a) Chen HM, Deng CH, Zhang XM. Angew Chem-Int Edit. 2010; 49:607.b) Liu J, Sun Z, Deng Y, Zou Y, Li C, Guo X, Xiong L, Gao Y, Li F, Zhao D. Angew Chem. 2009; 121:5989.c) Villanueva J, Philip J, Entenberg D, Chaparro CA, Tanwar MK, Holland EC, Tempst P. Anal Chem. 2004; 76:1560. [PubMed: 15018552] d) Shao HL, Min C, Issadore D, Liong M, Yoon TJ, Weissleder R, Lee H. Theranostics. 2012; 2:55. [PubMed: 22272219]
4. a) Lei C, Qian K, Noonan O, Nouwens A, Yu C. Nanoscale. 2013; 5:12033. [PubMed: 24162102] b) van Kampen JJ, Burgers PC, de Groot R, Gruters RA, Luider TM. Mass Spectrom Rev. 2011; 30:101. [PubMed: 20169623] c) Yates JR. Nat Methods. 2011; 8:633.d) Domon B, Aebersold R. Science. 2006; 312:212. [PubMed: 16614208]
5. a) Chiang CK, Chen WT, Chang HT. Chem Soc Rev. 2011; 40:1269. [PubMed: 21088773] b) Qiao L, Liu B, Girault HH. Nanomedicine. 2010; 5:1641. [PubMed: 21143038] c) Lin PC, Tseng MC, Su AK, Chen YJ, Lin CC. Anal Chem. 2007; 79:3401–3408. [PubMed: 17402709] d) Chen WY, Chen YC. Anal Bioanal Chem. 2006; 386:699. [PubMed: 16685517]
6. a) Martano G, Delmotte N, Kiefer P, Christen P, Kentner D, Bumann D, Vorholt JA. Nat Protoc. 2015; 10:1. [PubMed: 25474028] b) Kroemer G, Pouyssegur J. Cancer Cell. 2008; 13:472. [PubMed: 18538731]
7. Zenobi R. Science. 2013; 342:1201.
8. a) Hodgkinson CL, Morrow CJ, Li Y, Metcalf RL, Rothwell DG, Trapani F, Polanski R, Burt DJ, Simpson KL, Morris K, Pepper SD, Nonaka D, Greystoke A, Kelly P, Bola B, Krebs MG, Antonello J, Ayub M, Faulkner S, Priest L, Carter L, Tate C, Miller CJ, Blackhall F, Brady G, Dive C. Nat

Med. 2014; 20:897. [PubMed: 24880617] b) Lohr JG, Adalsteinsson VA, Cibulskis K, Choudhury AD, Rosenberg M, Cruz-Gordillo P, Francis JM, Zhang CZ, Shalek AK, Satija R, Trombetta JJ, Lu D, Tallapragada N, Tahirova N, Kim S, Blumenstiel B, Sougnez C, Lowe A, Wong B, Auclair D, Van Allen EM, Nakabayashi M, Lis RT, Lee GSM, Li T, Chabot MS, Taplin ME, Taplin ME, Clancy TE, Loda M, Regev A, Meyerson M, Hahn WC, Kantoff PW, Golub TR, Getz G, Boehm JS, Love JC. Nat Biotechnol. 2014; 32:479. [PubMed: 24752078] c) Lang JM, Casavant BP, Beebe DJ. Sci Transl Med. 2012; 4:4.d) Yu M, Stott S, Toner M, Maheswaran S, Haber DA. J Cell Biol. 2011; 192:373. [PubMed: 21300848]

9. Yu M, Bardia A, Aceto N, Bersani F, Madden MW, Donaldson MC, Desai R, Zhu HL, Comaills V, Zheng ZL, Wittner BS, Stojanov P, Brachtel E, Sgroi D, Kapur R, Shioda T, Ting DT, Ramaswamy S, Getz G, Iafrate AJ, Benes C, Toner M, Maheswaran S, Haber DA. Science. 2014; 345:216. [PubMed: 25013076]
10. a) Stott SL, Lee RJ, Nagrath S, Yu M, Miyamoto DT, Ulkus L, Inserra EJ, Ulman M, Springer S, Nakamura Z, Moore AL, Tsukrov DI, Kempner ME, Dahl DM, Wu CL, Iafrate AJ, Smith MR, Tompkins RG, Sequist LV, Toner M, Haber DA, Maheswaran S. Sci Transl Med. 2010; 2:10.b) Sarioglu AF, Aceto N, Kojic N, Donaldson MC, Zeinali M, Hamza B, Engstrom A, Zhu H, Sundaresan TK, Miyamoto DT, Luo X, Bardia A, Wittner BS, Ramaswamy S, Shioda T, Ting DT, Stott SL, Kapur R, Maheswaran S, Haber DA, Toner M. Nat Methods. 2015; 12:685. [PubMed: 25984697]
11. Stott SL, Hsu CH, Tsukrov DI, Yu M, Miyamoto DT, Waltman BA, Rothenberg SM, Shah AM, Smas ME, Korir GK, Floyd FP, Gilman AJ, Lord JB, Winokur D, Springer S, Irimia D, Nagrath S, Sequist LV, Lee RJ, Isselbacher KJ, Maheswaran S, Haber DA, Toner M. Proc Natl Acad Sci U S A. 2010; 107:18392. [PubMed: 20930119]
12. Li P, Mao ZM, Peng ZL, Zhou LL, Chen YC, Huang PH, Truica CI, Drabick JJ, El-Deiry WS, Dao M, Suresh S, Huang TJ. Proc Natl Acad Sci U S A. 2015; 112:4970. [PubMed: 25848039]
13. a) Plaks V, Koopman CD, Werb Z. Science. 2013; 341:1186. [PubMed: 24031008] b) Issadore D, Chung J, Shao HL, Liong M, Ghazani AA, Castro CM, Weissleder R, Lee H. Sci Transl Med. 2012; 4:10.
14. Riethdorf S, Fritsche H, Muller V, Rau T, Schindibeck C, Rack B, Janni W, Coith C, Beck K, Janicke F, Jackson S, Gornet T, Cristofanilli M, Pantel K. Clin Cancer Res. 2007; 13:920. [PubMed: 17289886]
15. a) Gan J, Wei X, Li Y, Wu J, Qian K, Liu B. Nanomedicine. 2015; 11:1715. [PubMed: 26169152] b) Qian K, Zhou L, Liu J, Yang J, Xu HY, Yu MH, Nouwens A, Zou J, Monteiro MJ, Yu CZ. Sci Rep. 2013; 3:7.
16. a) Wu CH, Huang YY, Chen P, Hoshino K, Liu H, Frenkel EP, Zhang JX, Sokolov KV. ACS nano. 2013; 7:8816. [PubMed: 24016305] b) Hoshino K, Huang YY, Lane N, Huebschman M, Uhr JW, Frenkel EP, Zhang XJ. Lab Chip. 2011; 11:3449. [PubMed: 21863182]
17. Deng Y, Qi D, Deng C, Zhang X, Zhao D. J Am Chem Soc. 2008; 130:28. [PubMed: 18076180]
18. a) Reátegui E, Aceto N, Lim EJ, Sullivan JP, Jensen AE, Zeinali M, Martel JM, Aranyosi AJ, Li W, Castleberry S. Adv Mater. 2015; 27:1593. [PubMed: 25640006] b) Earhart CM, Hughes CE, Gaster RS, Ooi CC, Wilson RJ, Zhou LY, Humke EW, Xu LY, Wong DJ, Willingham SB, Schwartz EJ, Weissman IL, Jeffrey SS, Neal JW, Rohatgi R, Wakeleebe HA, Wang SX. Lab Chip. 2014; 14:78. [PubMed: 23969419] c) Karabacak NM, Spuhler PS, Fachin F, Lim EJ, Pai V, Ozkumur E, Martel JM, Kojic N, Smith K, Chen PI, Yang J, Hwang H, Morgan B, Trautwein J, Barber TA, Stott SL, Maheswaran S, Kapur R, Haber DA, Toner M. Nat Protoc. 2014; 9:694. [PubMed: 24577360] d) Murlidhar V, Zeinali M, Grabauskiene S, Ghannad-Rezaie M, Wicha MS, Simeone DM, Ramnath N, Reddy RM, Nagrath S. Small. 2014; 10:4895. [PubMed: 25074448] e) Stott SL, Hsu CH, Tsukrov DI, Yu M, Miyamoto DT, Waltman BA, Rothenberg SM, Shah AM, Smas ME, Korir GK. Proc Natl Acad Sci. 2010; 107:18392. [PubMed: 20930119]
19. a) Li Z, Zhang YW, Xin YL, Bai Y, Zhou HH, Liu HW. Chem Commun. 2014; 50:15397.b) López de Laorden C, Beloqui A, Yate L, Calvo J, Puigivila M, Llop J, Reichardt N-C. Anal chem. 2014; 87:431. [PubMed: 25411795] c) Etxebarria J, Calvo J, Reichardt NC. Analyst. 2014; 139:2873. [PubMed: 24737011]

20. a) Qian K, Gu WY, Yuan P, Liu F, Wang YH, Monteiro M, Yu CZ. Small. 2012; 8:231. [PubMed: 22135224] b) Qian K, Wan JJ, Liu F, Girault HH, Liu BH, Yu CZ. ACS Nano. 2009; 3:3656. [PubMed: 19842678]
21. a) Zenobi R. Science. 2013; 342:1243259. [PubMed: 24311695] b) Chen EI, Hewel J, Krueger JS, Tiraby C, Weber MR, Kralli A, Becker K, Yates JR, Felding-Habermann B. Cancer res. 2007; 67:1472. [PubMed: 17308085]
22. Ooi HW, Cooper SJ, Huang CY, Jennins D, Chung E, Maeji NJ, Whittaker AK. Anal Biochem. 2014; 456:6. [PubMed: 24721294]
23. a) Qian K, Zhou L, Zhang J, Lei C, Yu CZ. Nanoscale. 2014; 6:5121. [PubMed: 24695592] b) Qian K, Wan JJ, Huang XD, Yang PY, Liu BH, Yu CZ. Chem-Eur J. 2010; 16:822. [PubMed: 20024995]
24. a) Shroff R, Rulisek L, Doubsky J, Svatos A. Proc Natl Acad Sci U S A. 2009; 106:10092. [PubMed: 19520825] b) Kim YK, Na HK, Kwack SJ, Ryoo SR, Lee Y, Hong S, Hong S, Jeong Y, Min DH. ACS Nano. 2011; 5:4550. [PubMed: 21539346]

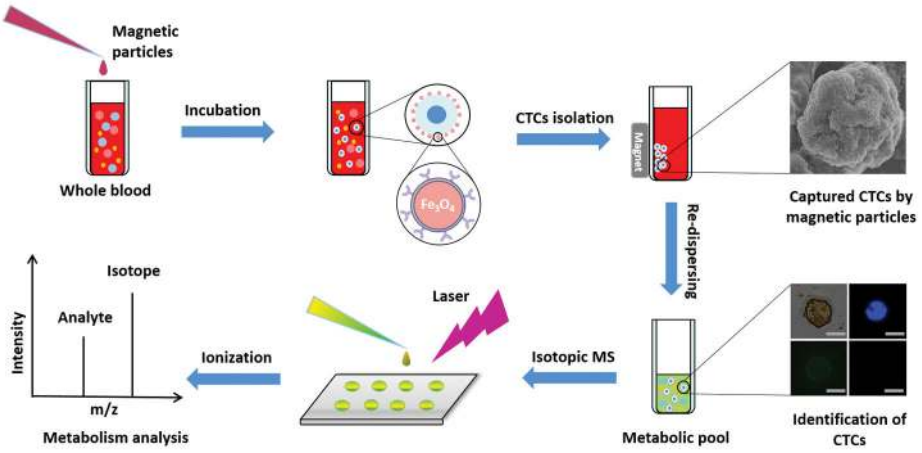

Figure 1.

Conceptual schematics of multi-functional magnetic particles based CTCs isolation and metabolism analysis using LDI MS.

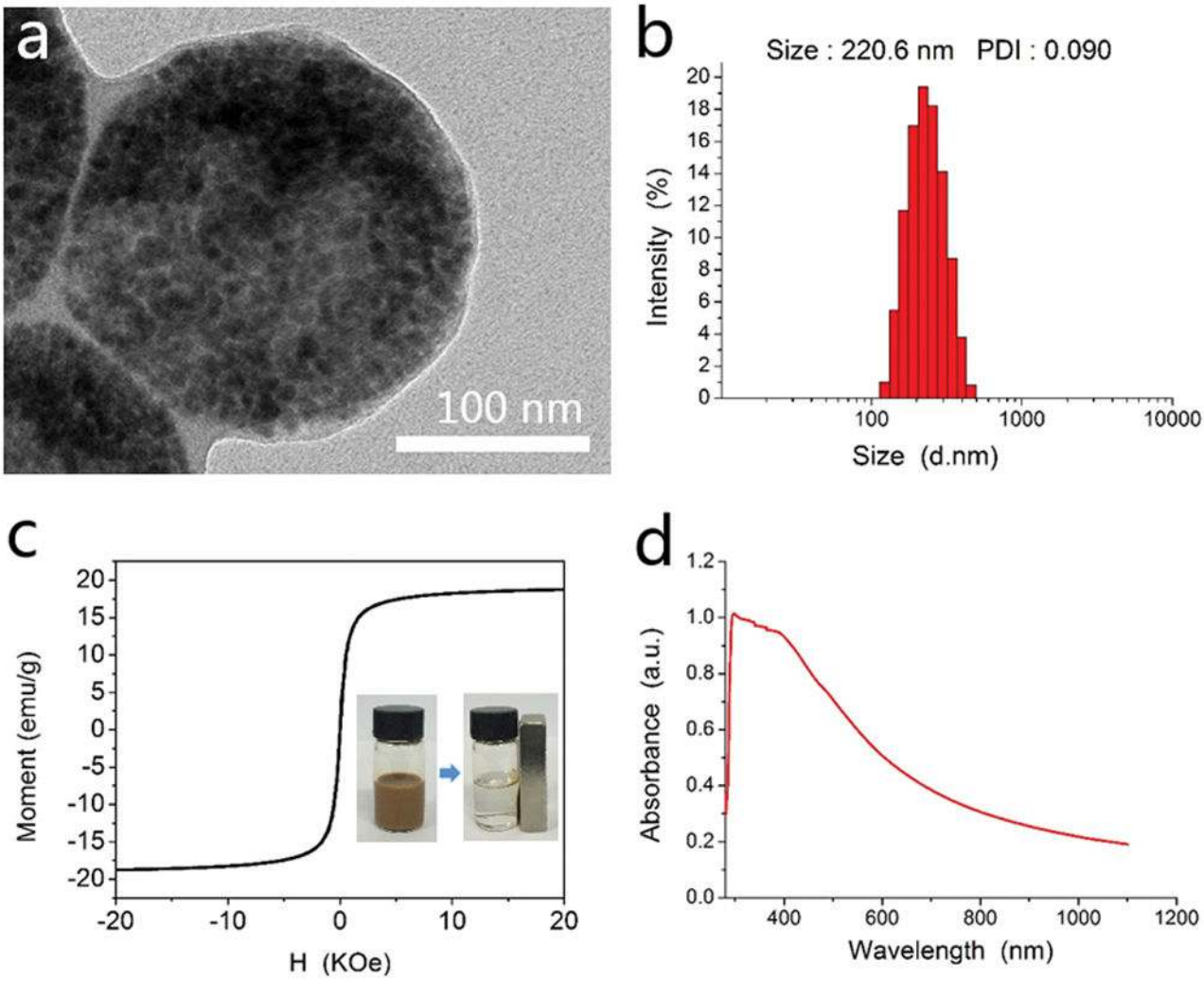

Figure 2.

Characterization of magnetic particles. (a) TEM and (b) particle size distributions and polydispersity index (PDI) of magnetic particles after anti-EpCAM modification. (c) Magnetic hysteresis loop of magnetic particles at 300K with inset showing magnetic response of particles from a colloidal suspension using a permanent magnet. (d) UV-vis absorption spectrum of magnetic particles after anti-EpCAM modification.

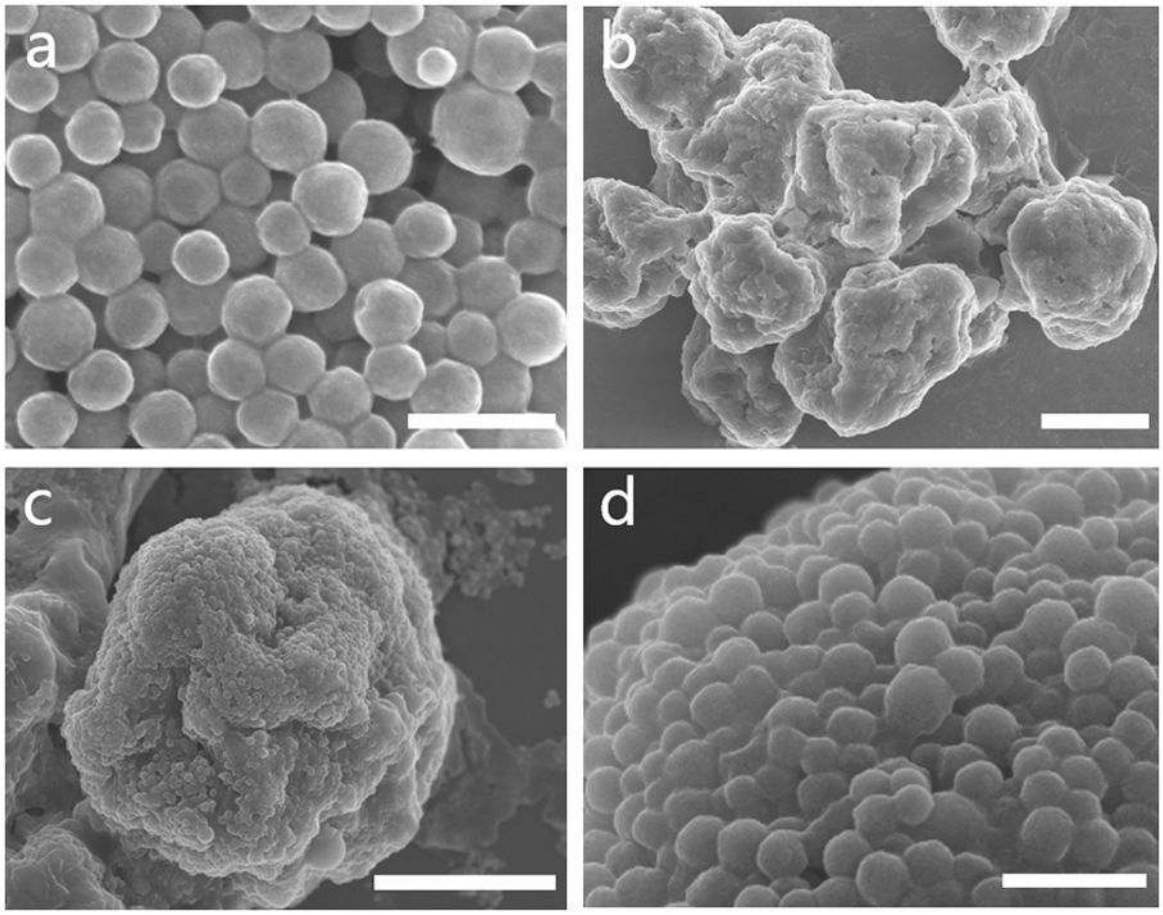

Figure 3.

Characterization of magnetic particles and as-captured cells. SEM images of (a) magnetic particles after anti-EpCAM conjugated on the surface and (b) pristine MCF-7 cells. SEM images of (c) captured MCF-7 cells coated by magnetic particles with (d) showing the surface of captured MCF-7 cells. The scale bar is 500 nm in (a) and (d), 5 μm in (b) and (c).

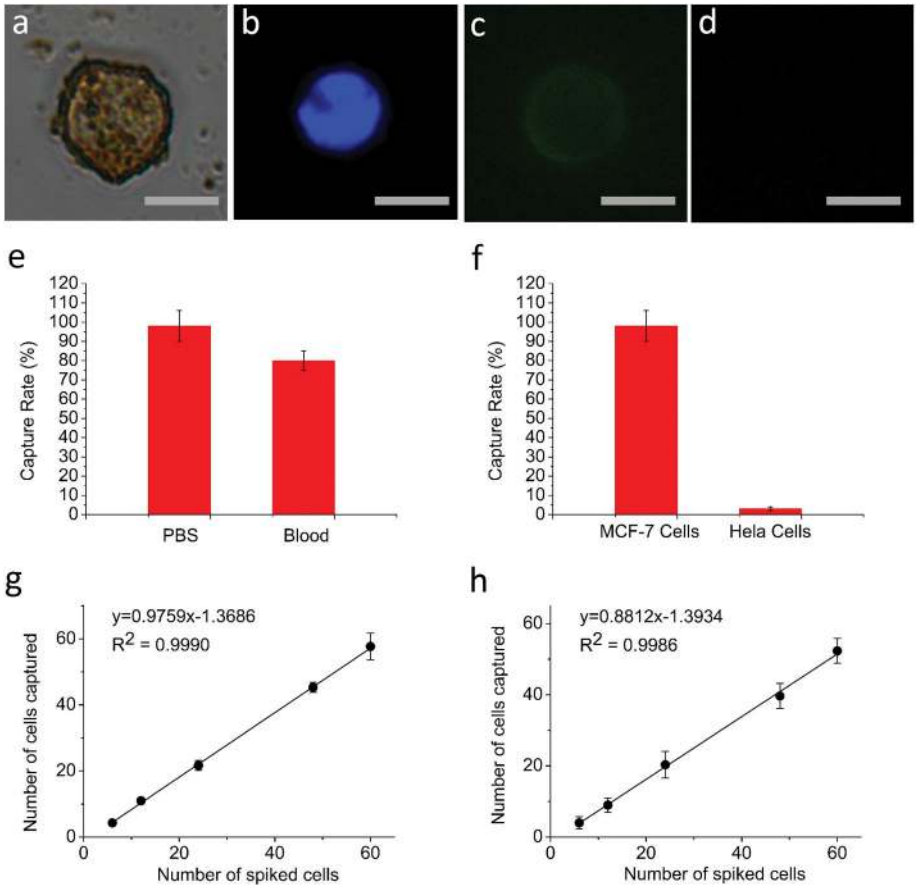

Figure 4.

Fluorescence staining images and capture efficiency of CTCs. (a) Bright field, and (b) DAPI (nucleus), (c) CK (FITC), and (d) CD45 (Cy3) fluorescence images of a captured MCF-7 cell. (e) Capture rate of anti-EpCAM modified magnetic particles in 2 mL of PBS and whole blood with 200 MCF-7 cells spiked; (f) comparison of capture rate between 200 MCF-7 (EpCAM positive) and 200 Hela (EpCAM negative) cells spiked in 2 mL of PBS using anti-EpCAM modified magnetic particles. The capture efficiency of CTCs using functional magnetic particles in (g) PBS and (h) whole blood spiked with different numbers of cells (concentrations ranging from 6 to 60 cells per mL). The scale bar is 10 μm in (a)–(d). Three independent experiments were performed with data shown in (e)–(g) as the mean ± s.d. (n = 3).

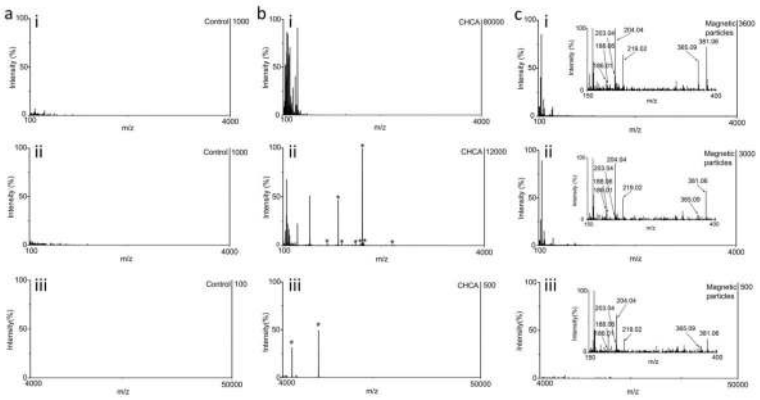

Figure 5.

LDI MS analysis of prepared bio-mixtures. LDI MS without matrix for (a-i) 0.5 μL solution containing 250 pmol glucose, sucrose, phenylalanine and glutamic acid; (a-ii) 0.5 μL of 1 mg/mL cytochrome c digested peptides mixed with 250 pmol glucose, sucrose, phenylalanine and glutamic acid; (a-iii) 0.5 μL of 10 mg/mL cytochrome c protein mixed with 250 pmol glucose, sucrose, phenylalanine and glutamic acid. LDI MS using CHCA for (b-i) 0.5 μL solution containing 250 pmol glucose, sucrose, phenylalanine and glutamic acid; (b-ii) 0.5 μL of 1 mg/mL cytochrome c digested peptides mixed with 250 pmol glucose, sucrose, phenylalanine and glutamic acid; (b-iii) 0.5 μL of 10 mg/mL cytochrome c protein mixed with 250 pmol glucose, sucrose, phenylalanine and glutamic acid. LDI MS using magnetic particles for (c-i) 0.5 μL solution containing 250 pmol glucose, sucrose, phenylalanine and glutamic acid; (c-ii) 0.5 μL of 1 mg/mL cytochrome c digested peptides mixed with 250 pmol glucose, sucrose, phenylalanine and glutamic acid; (c-iii) 0.5 μL of 10 mg/mL cytochrome c protein mixed with 250 pmol glucose, sucrose, phenylalanine and glutamic acid. The insets of (c-i, ii, iii) showed the low mass range of 100–400 Da. The * in (b-ii) stood for the identified peptides and the # in (b-iii) stood for observed protein signals.

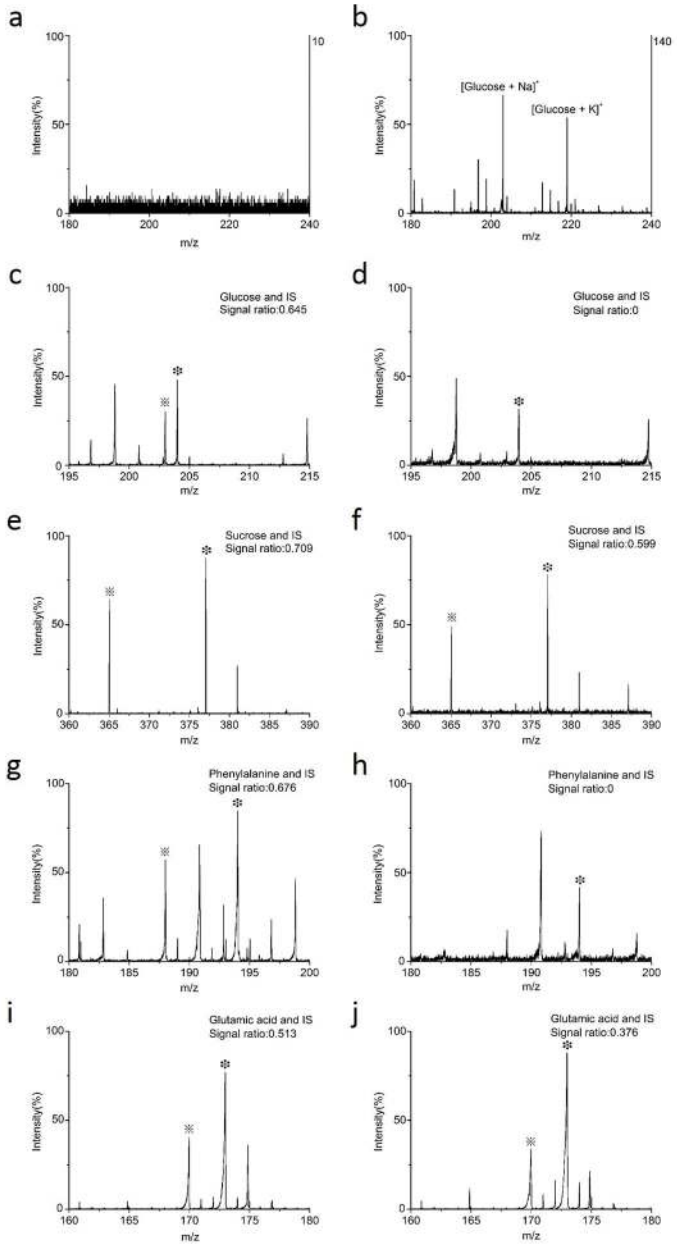

Figure 6.

LDI MS analysis of captured MCF-7 cells. MS spectra of (a) ~50 pristine MCF-7 cells without matrix and (b) ~50 captured MCF-7 cells in 100 ng/μL glucose. MS spectra of carbohydrates metabolites for glucose and internal standard (IS) isotope (c) before (0 h) and (d) after 24 h metabolic time; sucrose and IS isotope (e) before (0 h) and (f) after 24 h metabolic time. MS spectra of amino acids for phenylalanine and IS isotope (j) before (0 h) and (h) after 24 h metabolic time; glutamic acid and IS isotope (i) before (0 h) and (j) after 24 h metabolic time. The ※ represented metabolites and the ✻ represented corresponding IS isotopes in (c-j).

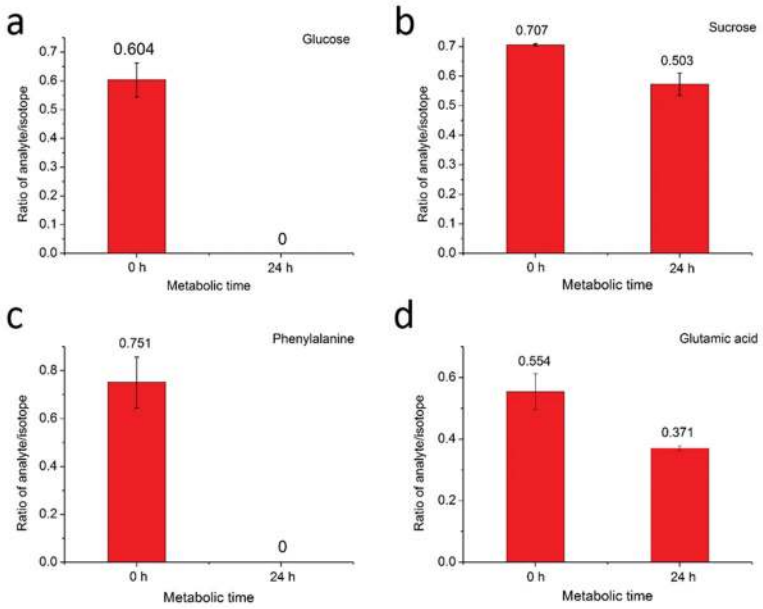

Figure 7.

Detection of CTCs metabolism. MS signal ratio of (a) glucose and IS isotope, (b) sucrose and IS isotope, (c) phenylalanine and IS isotope, and (d) glutamic acid and IS isotope for ~50 captured MCF-7 cells before (0 h) and after 24 h metabolic time. Five independent experiments were performed with data shown as the mean ± s.d. (n = 5).